PEROVSKITE SOLAR CELLS FABRICATION WITH PASSIVATION EFFECT OF HIGH MOBITITY PHENOTHIAZINE-BASED HOLE TRANSPORT LAYER

Adam Gajdos

Doctoral Degree Programme (4), FEEC BUT

E-mail: xgajdo12@vutbr.cz

Supervised by: Pavel Skarvada

E-mail: skarvada@feec.vutbr.cz

Abstract: Perovskite solar cells are today one of the hottest topics in photovoltaic devices. Compared to traditional c-Si, thin-film CIGS or CdTe solar cells, the fabrication of this type of solar cell is much cheaper, because production does not require ownership of a very expensive equipment and instrumentation. However, it has to be taken into account it has some initial issues as well as other newly developed technologies in the early stages of preparation for a commercial production. This paper deals with a newly synthesized hole transport material as a replacement of commercially available high-cost Spiro-OMETAD transport material. This commercial material has two main issues. Firstly, its production is very expensive and secondly it does not perform a function of a passivation layer for a sensitive perovskite layer. Our newly developed molecule has a positive effect on achieving long-term stable perovskite along with much cheaper production. The produced perovskite solar cell does not achieve highest power conversion efficiency, but they still look promising inf the view of long-term consistent performance.

Keywords: perovskite solar cell, fabrication, HTM, phenothiazine, passivation

1 INTRODUCTION

In the eight years since the first fabrication of all solid-state *perovskite solar cell* (PSC) by Nam Gyu Park et al. in 2012 [1], the *photoelectric conversion efficiencies* (PCEs) of PSCs have experienced an explosive growth. Certified PCEs of 25.2 % for small area PSCs with area of 0.0937 cm^2, have been achieved [2]. This remarkable achievement had led in PSCs to be considered the most promising class of third generation photovoltaic devices to replace the currently widely used Si solar cells.

Unfortunately, PCE is not main issues these days, there are several barriers remain to be overcome, (a) The environmental toxicity caused by the use of Pb in PSCs, (b) their unsatisfactory stability against temperature, humidity or light exposure, and (c) the dependence of their differential *J–V* characteristics on the scan directions [3]. Lead-free perovskites still have issue with high performance and there is a room for an improvement. Some hysteresis-free and stability towards temperature, humidity or light exposure PSCs achieved some improvements. In many cases, it was achieved by an interface passivation [4,5].

Interface passivation is the one of the most used and efficient strategies to improve the photovoltaic performance of perovskite solar cells (PSCs). According to *International Union of Pure and Applied Chemistry* (IUPAC), passivation, in physical chemistry and engineering, refers to a material becoming “passive”, that is, less affected or corroded by the environment in which it will be used. Passivation involves the application of an outer layer of a protective material as a micro coating, created by a chemical reaction with the base material. The transition process from the “active state” to the “passive state” by a formation of the passivating film. For perovskite solar cells, passivation generally refers to either chemical passivation, which reduces the trap states caused by defects in order to

optimize the charge transfer between various interfaces [6] or physical passivation, which isolates certain functional layers from the external environment to avoid degradation of the device.

Typical PSCs contain six main interfaces, including (a) the interface between the *transparent conductive oxide* (TCO) and *electron transport layer* (ETL); (b) the interface between the ETL and perovskite; (c) the interface between the grains of perovskite itself (i.e. grain boundaries); (d) the interface between the perovskite and *hole transport layer* (HTL); (e) the interface between the HTL and electrode, and (f) the interface between the electrode material and atmospheric environment [7].

2 RESULTS AND DISCUSSION

2.1 PHENOTHIAZINE-BASED ORGANIC SEMICONDUCTOR

A novel push-pull para-methoxyphenyl N-substituted phenothiazine-based organic semiconductor (O-1) published in [8] was used as *hole transport material* (HTM) as well as a passivation interface on the perovskite layer. Chemical structure of the molecule itself is illustrated in **Figure 1**. Electrochemical, optical and thermal properties of molecule O-1, which is reported in [8], show off perfect suitability for organic electronic applications.

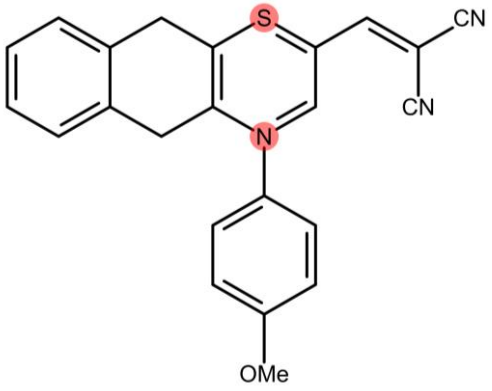

Figure 1: Chemical structure of the phenothiazine derivative O-1.

Outstanding charge carrier mobility of 1×10^{-3} cm^2 V^{-1} s^{-1}, the highest reported for this class of compounds, correlates with some significant characteristics determining the performance of organic electronic devices. Hole mobility of O-1 compared to Spiro-OMETAD (standard compound for perovskite solar cells fabrication as HTM) is almost by two orders higher. The *highest occupied molecular orbital* (HOMO) level, corresponding to the ionization potentials of the materials, were derived from *differential pulse voltammetry* (DPV) in dichloromethane solution. The highest occupied molecular orbital level of O-1 is −5.29 eV, which is slightly lower than HOMO level of Spiro-OMETAD.

The *ultraviolet-visible* (UV-Vis) absorption spectra of O-1 thin films are shown in **Figure 2**a. The molecule O-1 were dissolved in *chlorobenzene* (CB) with a concentration of 10 mg ml^{-1} and 34 mg ml^{-1}, and spin-coated onto glass substrates. Naturally, the higher concentration leads to a higher absorption. The absorption spectra show in Figure 2a two distinct bands. One band is at wavelength of 334 nm and another at 506 nm.

Thermal properties of O-1 were investigated with *differential scanning calorimetry* (DSC) and *thermogravimetric analysis* (TGA). The results of DSC shown *melting temperature* (T_m) point at 199 °C and *decomposition temperature* (T_d) at 302 °C was obtained from TGA [8].

Figure 2b presents photoluminescence emission spectra of the perovskite film on glass (excitation wavelength at 640 nm). Addition of Spiro-OMETAD results in notable spectral change, local excited state emission at 780 nm is almost quenched (97,1 %). Addition of O-1 results in 86,7% quenching of excited state.

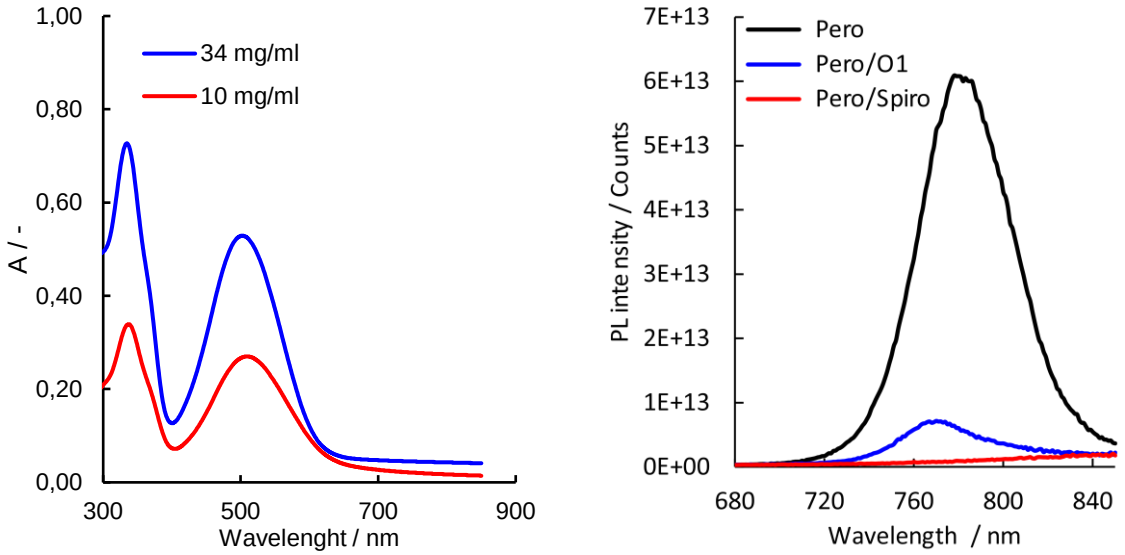

Figure 2: (a) UV-Vis absorption spectra of freshly prepared films of O-1 molecule; (b) Photoluminescence (PL) spectra of a perovskite film (black line), a perovskite film with Spiro-MeOTAD (red line), and a perovskite film with a O-1 (blue line).

2.2 DEVICE FABRICATION

Fluorine-doped Tin Oxide (FTO) glass substrates were etched in the mixture of Zn powder and 4M *hydrochloric acid* (HCl) to define active area and prevent short circuit from top Au electrode directly to FTO. Four step ultrasonication bath procedure in 2% Mucasol, deionized water, acetone and isopropanol were performed after etching ended up by a nitrogen flow drying.

After cleaning, UV ozone was used right before *compact titanium dioxide* (c-TiO_2) layer were deposited by spray pyrolysis. Clean substrates were placed onto hotplate and left for 15 minutes at temperature of 450 °C. The precursor solution comprises 0.45 ml of acetylacetone and 0.70 ml of titanium diisopropoxide bis(acetylacetonate) stock solution (75% in 2-propanol) diluted in 9 ml of ethanol. The whole solution is sprayed using oxygen as carrying gas at a distance of 15 cm, with at least 30 s of delay between each spraying cycle. During each cycle all the FTO surface must be covered within few seconds. After spraying, substrates are maintained at temperature of 450 °C for an additional 20 min before cooldown [9].

Mesoporous titanium dioxide (m-TiO_2) layer was spin-coated. The solution of 30 N-RD Dyesol TiO_2 paste diluted under stirring as 150 mg ml^{-1} of ethanol should be prepared at least one day before using it and left under stirring all the time. Spin-coater is set to 4000 rpm with an acceleration of 2000 rpm s^{-1} for 10 s, after spinning substrates are sintered at temperature of 450 °C for 30 min, then cooled down to room temperature [9].

Perovskite film deposition is multiple step procedure. One day before film deposition, we prepare 1.5M PbI_2 and 1.5M $PbBr_2$ stock solutions in 4:1 V/V dimethylformamide (DMF)/dimethyl sulfoxide (DMSO) mixture and 1.5M CsI stock solution in DMSO and let them warmed overnight at 65 °C. Next day, we prepare 1.27M bromide MABr:$PbBr_2$ (MaPbBr3) and 1.27M iodine FAI:PbI_2 ($FAPbI_3$) based perovskite solutions and mix them in a 5:1 V/V ratio. By mixing, we get the MAFA precursor solution with the nominal formula of $(FAPbI_3)_{83}$ $(MAPbBr_3)_{17}$. Final step for CsMAFA precursor is addition of CsI stock solution to MAFA precursor in 5:95 V/V. Perovskite film is deposited by two-step static spin-coating in glovebox, first step (10 s at 1000 rpm with 200 rpm s^{-1}) to ensure full surface coverage after dropping 100 µl the solution in the middle of the substrate and a second step (20 s at 6000 rpm with 2000 rpm s^{-1}), 5 s before end of spinning dispense 100 µl of chlorobenzene (the antisolvent). Immediately after spinning ends place substrate on the hot plate at temperature of 100 °C for 60 mins [9].

The O-1 solution was prepared in two different concentrations, 10 mg ml^{-1} and 20 mg ml^{-1}. The powder O-1 was diluted in CB and preheated to 120 °C. Film was deposited by dynamic spin-coating with equal parameters of spin-coater to Spiro-OMETAD deposition step (30 s at 1800 rpm), after deposition the substrates rest overnight in dry air.

Gold layer is evaporated as a top selective electrode and it is deposited in a two-step process: the first 2 nm at 0.1 Å s^{-1} and then at 1.2 Å s^{-1} up to 100 nm. The schematic and corresponding SEM cross-section images are shown in **Figure 3**.

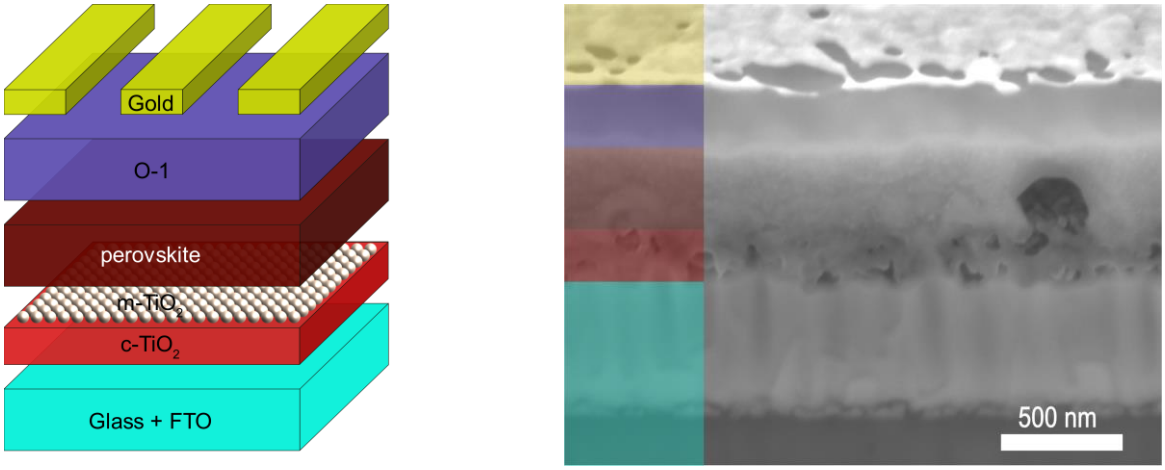

(a) (b)

Figure 3: (a) Schematic of perovskite solar cell architecture. (b) The corresponding SEM cross-section image is shown below with a scale bar of 500 nm. Part of the SEM image have been coloured following the schematic.

2.3 DEVICE PERFORMANCE

Produced batch consist of 12 samples, each sample comprise of 4 devices (6 samples with 10 mg ml^{-1} O-1 and 20 mg ml^{-1}). Nevertheless, none of samples using 20 mg ml^{-1} O-1 concentration perform properly, *power conversion efficiency* (PCE) was always less than 1 %. It can be caused by several circumstances (too thick layer for charge transport, also it may be caused with same soluble problem which O-1 had). Figure 4a shows *fill factor* (FF) and PCE of all devices which using 10 mg ml^{-1} O-1. Average fill factor is 40,5 %, avg. PCE is 4,5 %. *J*–*V* plot for sample S3E3 is depicted in Figure 4b, it shows hysteresis effect in forward and backward scan. All *J*–*V* data have been collected with 10 mV s^{-1} scanning rate.

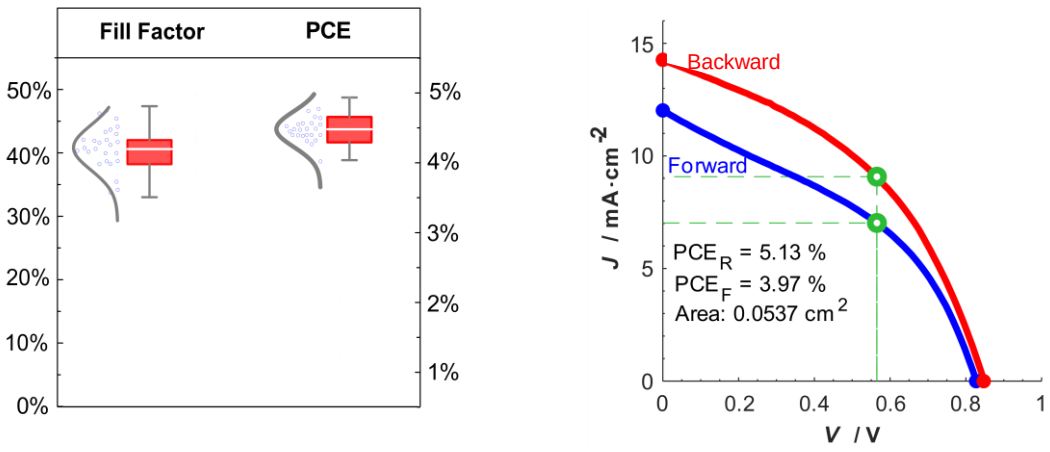

(a) (b)

Figure 4: (a) The fill factor and power conversion efficiency values for PSCs with 10 mg ml^{-1} O-1, box plots shown alongside the corresponding data points for one batch of fabricated samples. (b) *J*–*V* characteristics for sample S3E3 in forward and backward scan.

3 CONCLUSION

We reported addition initial characterization of newly synthesized molecule O-1 to prove suitability for HTM application in perovskite solar cells. Photoluminescence spectra shows 86.7 % quenching with CsMAFA perovskite film, which is not good as Spiro-OMETAD, but still suitable for HTM application. Fabrication process have been reported briefly, because it is almost similar procedure published in [9]. However, some small modifications have been made and of course novelty in O-1 precursor application as HTM**,** which was not published at all. Fill factor and power conversion efficiency for all fabricated samples were calculated from *J–V* measurements done on Sciencetech SS150 AAA solar simulator, which was calibrated to 1 sun. Highest measured efficiency was 5.13 % with fill factor 42.44 %.

ACKNOWLEDGEMENT

This work was supported by the Internal Grant Agency of Brno University of Technology, grant No. FEKT-S-20-6352. This support was gratefully acknowledged.

REFERENCES

[1] Kim H-S, Lee C-R, Im J-H, Lee K-B, Moehl T, Marchioro A, Moon S-J, Humphry-Baker R, Yum J-H, Moser J E, Grätzel M and Park N-G 2012 Lead iodide perovskite sensitized all-solid-state submicron thin film mesoscopic solar cell with efficiency exceeding 9% *Scientific Reports* **2**

[2] Jung E H, Jeon N J, Park E Y, Moon C S, Shin T J, Yang T-Y, Noh J H and Seo J 2019 Efficient, stable and scalable perovskite solar cells using poly(3-hexylthiophene) *Nature* **567** 511–5

[3] van Reenen S, Kemerink M and Snaith H J 2015 Modeling Anomalous Hysteresis in Perovskite Solar Cells *J. Phys. Chem. Lett.* **6** 3808–14

[4] Han F, Luo J, Zhao B, Wan Z, Wang R and Jia C 2017 Cesium Iodide Interface Modification for High Efficiency, High Stability and Low Hysteresis Perovskite Solar Cells *Electrochimica Acta* **236** 122–30

[5] Chaudhary B, Kulkarni A, Jena A K, Ikegami M, Udagawa Y, Kunugita H, Ema K and Miyasaka T 2017 Poly(4-Vinylpyridine)-Based Interfacial Passivation to Enhance Voltage and Moisture Stability of Lead Halide Perovskite Solar Cells *ChemSusChem* **10** 2473–9

[6] Arora N, Dar M I, Abdi-Jalebi M, Giordano F, Pellet N, Jacopin G, Friend R H, Zakeeruddin S M and Grätzel M 2016 Intrinsic and Extrinsic Stability of Formamidinium Lead Bromide Perovskite Solar Cells Yielding High Photovoltage *Nano Lett.* **16** 7155–62

[7] Anon Impact of Interfacial Layers in Perovskite Solar Cells - Cho - 2017 - ChemSusChem - Wiley Online Library

[8] Shinde D B, Salunke J K, Candeias N R, Tinti F, Gazzano M, Wadgaonkar P P, Priimagi A, Camaioni N and Vivo P 2017 Crystallisation-enhanced bulk hole mobility in phenothiazine-based organic semiconductors *Sci Rep* **7** 1–10

[9] Saliba M, Correa-Baena J-P, Wolff C M, Stolterfoht M, Phung N, Albrecht S, Neher D and Abate A 2018 How to Make over 20% Efficient Perovskite Solar Cells in Regular (n–i–p) and Inverted (p–i–n) Architectures *Chem. Mater.* **30** 4193–201